

Discovery of Novel 4-Arylisochromenes as Anticancer Agents Inhibiting Tubulin Polymerization

Wenlong Li, Wen Shuai, Feijie Xu, Honghao Sun, Shengtao Xu, Hong Yao, Jie Liu, Hequan Yao, Zheyang Zhu, and Jinyi Xu

ACS Med. Chem. Lett., **Just Accepted Manuscript** • DOI: 10.1021/acsmedchemlett.8b00217 • Publication Date (Web): 25 Sep 2018

Downloaded from <http://pubs.acs.org> on September 26, 2018

Just Accepted

"Just Accepted" manuscripts have been peer-reviewed and accepted for publication. They are posted online prior to technical editing, formatting for publication and author proofing. The American Chemical Society provides "Just Accepted" as a service to the research community to expedite the dissemination of scientific material as soon as possible after acceptance. "Just Accepted" manuscripts appear in full in PDF format accompanied by an HTML abstract. "Just Accepted" manuscripts have been fully peer reviewed, but should not be considered the official version of record. They are citable by the Digital Object Identifier (DOI®). "Just Accepted" is an optional service offered to authors. Therefore, the "Just Accepted" Web site may not include all articles that will be published in the journal. After a manuscript is technically edited and formatted, it will be removed from the "Just Accepted" Web site and published as an ASAP article. Note that technical editing may introduce minor changes to the manuscript text and/or graphics which could affect content, and all legal disclaimers and ethical guidelines that apply to the journal pertain. ACS cannot be held responsible for errors or consequences arising from the use of information contained in these "Just Accepted" manuscripts.



Discovery of Novel 4-Arylisochromenes as Anticancer Agents Inhibiting Tubulin Polymerization

Wenlong Li^a, Wen Shuai^a, Feijie Xu^a, Honghao Sun^a, Shengtao Xu^{a,*}, Hong Yao^a, Jie Liu^{b,*}, Hequan Yao^a, Zheyang Zhu^c, Jinyi Xu^{a,*}

^aDepartment of Medicinal Chemistry and State Key Laboratory of Natural Medicines, China Pharmaceutical University, 24 Tong Jia Xiang, Nanjing 210009, P. R. China

^bDepartment of Organic Chemistry, China Pharmaceutical University, 24 Tong Jia Xiang, Nanjing 210009, P. R. China

^cDivision of Molecular Therapeutics & Formulation, School of Pharmacy, The University of Nottingham, University Park Campus, Nottingham NG7 2RD, UK

KEYWORDS: *Combretastatin A-4*, *(±)-7,8-Dihydroxy-3-methylisochroman-4-one*, *Tubulin inhibitors*, *Enantioseparation*, *Anti-tumor*, *Vascular disrupting*

ABSTRACT: XJP-L (**8**), a derivative of the natural product *(±)-7,8-dihydroxy-3-methylisochroman-4-one* isolated from the peel of *Musa sapientum L.*, was found to exhibit weak inhibitory activity of tubulin polymerization ($IC_{50} = 10.6 \mu M$) in our previous studies. Thus, a series of 4-arylisochromene derivatives were prepared by incorporating the trimethoxyphenyl moiety into **8**. Among which, compound *(±)-19b* was identified as the most potent compound with IC_{50} values ranging from 10 to 25 nM against a panel of cancer cell lines. Further mechanism studies demonstrated that *(±)-19b* disrupted the intracellular microtubule network, caused G2/M phase arrest, induced cell apoptosis and depolarized mitochondria of K562 cells. Moreover, *(±)-19b* exhibited potent *in vitro* anti-vascular and *in vivo* anti-tumor activities. Notably, the *R*-configured enantiomer of *(±)-19b*, which was prepared by chiral separation, was slightly more potent than *(±)-19b* and was much more potent than the *S*-configured enantiomer in both anti-proliferative and anti-tubulin assays. Our findings suggest that *(±)-19b* deserves further research as a potential anti-tubulin agent for the treatment of cancers.

Combretastatin A-4 (**1**, CA-4) (Figure 1), a natural *cis*-stilbene derivative isolated from the bark of the African willow tree *Combretum caffrum*,¹ was found to be a powerful inhibitor of tubulin polymerization targeting the colchicine binding site.² CA-4 has strong cytotoxicity against a variety of tumor cells with a broad therapeutic window. Besides, CA-4 was reported to show vascular disrupting properties at a tolerated dose.³ The potent antimitotic and vascular disrupting profiles of CA-4 made it a promising therapy for the treatment of cancers.⁴⁻⁷ However, CA-4P (**2**, Fosbretabulin), the phosphate prodrug of CA-4, had been discontinued in clinical trials⁸ due to the lack of a meaningful improvement in progression-free survival (PFS) and unfavorable partial response data.⁹ In the presence of light, heat or acid media, but also after *in vivo* administration, the *Z*-isomer of CA-4 easily isomerizes to the *E*-isomer that is significantly less potent at inhibiting tubulin polymerization and cancer cell growth.¹⁰ Strategies to surmount this drawback have been taken by modification on the bridge structure of CA-4, which lead to the discovery of various moieties replacing the *cis*-double bond.¹¹⁻¹³ Fusing *cis*-olefin into the ring B represents an important tactic to lock the

cis double bond, compounds **3-6** with highly potent cytotoxicity were thus discovered (Figure 1).¹⁴⁻²¹

It is known to all that natural products with structurally diverse frameworks have always been and continue to be an important source for new drug discovery.²² *(±)-7,8-Dihydroxy-3-methylisochroman-4-one* [**7**, *(±)-XJP*] was a structurally unique 4-isochromanone compound which was isolated from the peel of *Musa sapientum L.* and total synthesized by our group,^{23,24} and it exhibited a wide range of favorable pharmacological properties.^{25,26} In our previous research for discovering new anti-tubulin agents with novel skeletons, a series of XJP derivatives was screened for their inhibitory activity of tubulin polymerization. Interestingly, XJP-L (**8**) was found to exhibit weak microtubule polymerization inhibitory activity ($IC_{50} = 10.6 \mu M$).

Considering the vital roles of 3,4,5-trimethoxyphenyl on the activity of inhibitors of tubulin polymerization targeting the colchicine binding site,²⁷⁻²⁹ **8** was further hybridized with 3,4,5-trimethoxyphenyl moiety for improving both its anti-proliferative and inhibitory activities of tubulin polymerization using the *cis*-double bond locking strategy. Thus, a series of

novel 4-arylisochromenes were designed and synthesized (Figure 1). Herein, we wish to report their synthesis and anti-tumor activities as anti-tubulin agents.

The synthetic route for the preparation of 4-arylisochromenes is outlined in Scheme 1. Various substituted XJP scaffolds **12a-e** were synthesized according to the method utilizing a Parham-type cyclization with the *tert*-butyllithium reagent reported by our group.³⁰ Sulphur-containing XJP scaffolds **12f-g** were further synthesized via a Friedel-Crafts cyclic reaction.

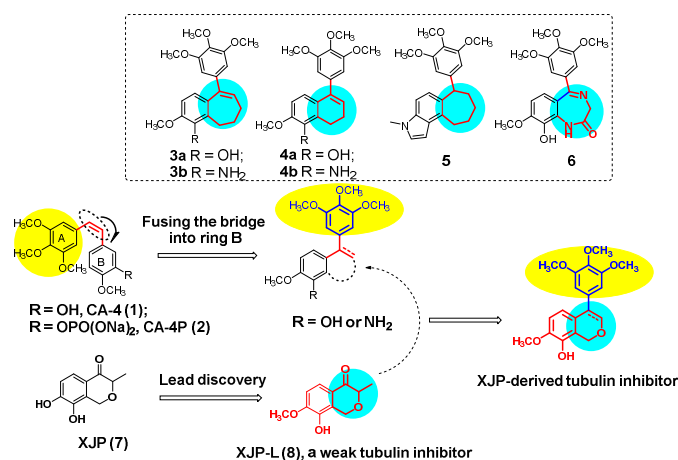


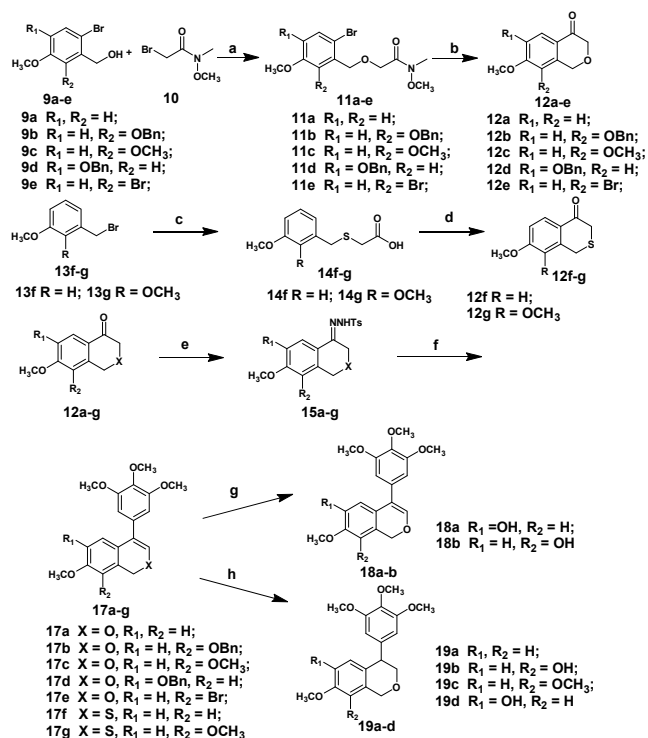
Figure 1. The strategy of fusing the bridge into ring B of CA-4 to surmount its instability and the design of XJP derived tubulin inhibitor.

Then, **12a-g** were transformed into their corresponding *N*-tosylhydrazones **15a-g** in refluxing EtOH with good to excellent yields, followed by the coupling of **15a-g** with 5-bromo-1,2,3-trimethoxybenzene (**16**) via a Pd-catalyzed cross-coupling to afford **17a-g** in moderate to good yields. Utilizing the different reducing capacity of Pd-C/H₂ in THF and CH₃OH, benzyl group of **17b** and **17d** were selectively deprotected using THF as the solvent to give compound **18a** and **18b**, respectively, while double bonds were reduced to afford (±)-**19a-d** with CH₃OH as the solvent.

All target compounds **17a**, **17c**, **17e-g**, **18a-b** and (±)-**19a-d** were initiatively evaluated for their anti-proliferative activities against human hepatocellular carcinoma cells (HepG2) by the MTT assays. Most of the synthesized compounds displayed potent activity against HepG2 cells and the preliminary structure activity relationships (SARs) were obtained. The position of hydroxyl group on the isochroman moiety was crucial for anti-proliferative activity. Compound **18b** and (±)-**19b**, which contain hydroxyl at the C-5 position (R₂), exhibited the most potent activity with IC₅₀ values of 26 and 15 nM, respectively. Moving the OH group from C-5 position to C-3 position led to the loss of anti-proliferative activity (**18a** and **19d**, IC₅₀ > 10 μM). When R₂ was substituted with other groups such as OCH₃ [**17c** and (±)-**19c**], Br (**17e**) or no substitution [**17a** and (±)-**19a**], the activity significantly decreased when compared with **18b** and (±)-**19b**. Besides, the activity was maintained when sulfur (X = S) was introduced into the isochroman scaffold (**17f** and **17g**). The reduction of double bonds led to a

slightly improvement of activity [**17a** vs **19a**, **17c** vs (±)-**19c** and **18b** vs (±)-**19b**]. Especially, compound (±)-**19b** displayed the most potent anti-proliferative activity (IC₅₀ = 15 nM), which exhibited nearly 1000-fold improvement of activity towards **8** (IC₅₀ = 23.7 μM) (See Supporting Information Table S1).

Scheme 1. Synthetic route to 4-arylisochromenes^a



^aReagents and conditions: (a) NaH, DMF, 2h, 55-70%; (b) *t*-BuLi, THF, -78 °C, 15min, 72-90%; (c) i) ethyl thioglycolate, K₂CO₃, CH₃CN, 2h, 75-88%; ii) 10% NaOH aqueous, CH₃OH, 80 °C, 85-90%; (d) i) oxalyl chloride, DMF(cat.), DCM; ii) SnCl₄, chlorobenzene, 55-65% over two steps; (e) *p*-Toluenesulfonylhydrazide, EtOH, 90 °C, 75-90%; (f) 5-bromo-1,2,3-trimethoxybenzene (**16**), PdCl₂(CH₃CN)₂, Xphos, *t*-BuOLi, 90 °C, 45-70%; (g) Pd/C, H₂, THF, 65-92%; (h) Pd/C, H₂, CH₃OH, 72-95%.

Subsequently, compounds **18b** and (±)-**19b** were further evaluated for their anti-proliferative activity against another five cancer cell lines including KB, HCT-8, MDA-MB-231, K562 and H22 cells. As shown in Table 1, both **18b** and (±)-**19b** showed potent anti-proliferative activities. Especially, (±)-**19b** exhibited the most active against K562 cell lines with the IC₅₀ value of 10 nM, which is more potent than the positive control CA-4 (IC₅₀ = 15 nM); Human normal hepatocytes LO2 cells were also used to determine their selectivity towards cancer cells and normal cells, which showed that **18b** and (±)-**19b** selectively inhibited the growth of cancer cells.

The further *in vitro* assay for the inhibition of tubulin polymerization demonstrated that compounds **18b** and (±)-**19b** were potent inhibitors of tubulin polymerization. As shown in Table 1, compound (±)-**19b** (IC₅₀ = 3.1 μM) was more potent than **18b** (IC₅₀ = 4.2 μM) and was slightly less potent than CA-

Table 1. Cytotoxicity against five cancer cell lines, Human normal hepatocytes LO2 cells and ITP of compounds 18b, (±)-19b, (R)-(+)-19b and (S)-(-)-19b^a

Compd.	IC ₅₀ values (μM)						
	KB	HCT-8	MDA-MB-231	K562	H22	LO2	ITP ^b
18b	0.016±0.002	0.025±0.004	0.028±0.004	0.019±0.002	0.010±0.001	0.138±0.012	4.2±0.3
(±)-19b	0.025±0.002	0.030±0.002	0.022±0.002	0.010±0.001	0.011±0.001	0.095±0.010	3.1±0.2
(R)-(+)-19b	0.012±0.002	0.012±0.001	0.011±0.002	0.008±0.001	0.008±0.002	0.058±0.005	2.5±0.1
(S)-(-)-19b	0.87±0.08	0.94±0.12	0.90±0.09	0.46±0.06	0.80±0.12	0.90±0.08	4.3±0.1
CA-4	0.012±0.001	0.015±0.002	0.015±0.002	0.015±0.002	0.008±0.001	0.095±0.002	2.5±0.2
8	25.1±0.9	35.2±1.3	30.2±2.0	20.5±1.2	18.2±2.1	22.2±1.2	10.6±0.2

^aMTT methods; cells were incubated with indicated compounds for 72 h (means ± SD, n = 3).
^bInhibition of tubulin polymerization activity.

-4 (IC₅₀ = 2.5 μM). Furthermore, (±)-19b exhibited nearly 3-fold improvement of inhibitory activity of tubulin polymerization compared with 8 (IC₅₀ = 10.6 μM), which suggested that the trimethoxyphenyl moiety has significant roles in binding with tubulin. In addition, in assay of the colchicine competitive experiment, the binding potency of (±)-19b to the colchicine binding site was comparable to that of CA-4 with the inhibition rates of 76.4% and 89.6% at 1 μM and 5 μM, respectively (see Supporting Information Table S2), indicating that (±)-19b binds to the colchicine binding site.

Moreover, immunofluorescent assays were performed to investigate the effect of (±)-19b on microtubule networks. As shown in Figure 2, K562 cells exhibited normal filamentous microtubules arrays without drug treatment. However, after exposure to (±)-19b at three different concentrations (5 nM, 10 nM, 20 nM) for 24 h, the microtubule networks in cytosol were disrupted, indicating that (±)-19b induced a dose-dependent collapse of the microtubule networks.

Since most microtubule polymerization inhibitors disrupt cell mitosis and exert cell cycle arrest effects,³¹ the effect of (±)-19b on cell cycle progression using propidiumiodide (PI) staining in K562 cells was examined. When treated with (±)-19b at 5 nM, 10 nM, 20 nM for 48 h, the percentages of cells arrested at the G2/M phase were 17.5%, 19.5%, and 22.4%, respectively, indicating that (±)-19b can disrupt the dynamic balance of the tubulin-microtubule system and further induced the cell cycle arrest at the G2/M phase (see Supporting Information Figure S1). Next, an Annexin V-APC/7-AAD binding assay was carried out to assess whether (±)-19b would induce cell apoptosis. The percentage of apoptotic cells after the 48 h treatment was only 5.7% in the control group. The total numbers of early (Annexin-V+/PI-) and late (Annexin-V+/PI+) apoptotic cells increased to 13.7%, 29.0% and 54.1% after treatment with (±)-19b at 5, 10, 20 nM for 48 h, respectively (see Supporting Information Figure S2). These results confirmed that (±)-19b effectively induced cell apoptosis in K562 cells in a dose-dependent manner.

In order to determine whether (±)-19b-induced apoptosis was involved in a disruption of mitochondrial membrane integrity, the fluorescent probe JC-1 was employed to measure the mitochondrial membrane potential (MMP). When treated

with (±)-19b at concentrations of 0, 5, 10 and 20 nM for 48 h, the number of K562 cells with collapsed MMP increased to 0.6%, 12.7%, 26.7% and 55.1%, respectively (see Supporting Information Figure S3), suggesting that (±)-19b caused mitochondrial depolarization of K562 cells in the process of apoptosis.

Most microtubule binding agents have antiangiogenic or vascular-disrupting activities or both, which are anti-vascular effects.³² Angiogenesis inhibiting agents (AIAs) interfere with new vessel formation, require chronic administration, and are likely to be of benefit in early-stage or asymptomatic metastatic disease. While vascular-disrupting agents (VDAs) target the

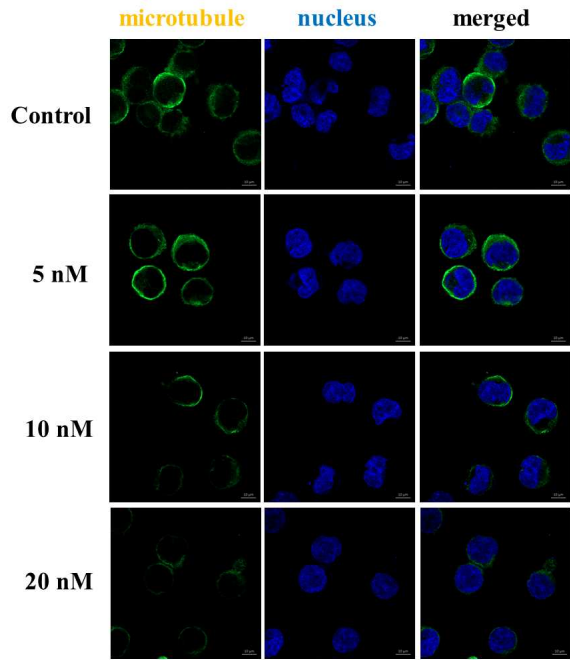


Figure 2. Effects of (±)-19b on the cellular microtubule network visualized by immunofluorescence.

established tumor blood vessels, which are often given acutely and have particular efficacy against advanced disease.³³ Con-

sidering that invasion and tube formation are highly relevant properties in the process of tumor vasculature, the HUVEC culture assay was used to assess the ability of (\pm)-**19b** to inhibit HUVEC migration. As a result, the untreated cells migrated to fill the area that was initially scraped after 24 h. In contrast, (\pm)-**19b** significantly inhibited the HUVEC migration in a dose-dependent manner (see Supporting Information Figure S4A). Then we further evaluated the anti-vascular ability of (\pm)-**19b** in a tube formation assay. After being seeded on matrigel, HUVECs form the capillary-like tubules with multicentric junctions. After exposure to (\pm)-**19b** at doses of 0, 5, 10, and 20 nM for 6 h, the capillary-like tubes were interrupted in different levels (Figure S4B). These results showed that (\pm)-**19b** effectively inhibited the tube formation of HUVECs.

Furthermore, we tested the *in vivo* anti-tumor activity of (\pm)-**19b** based on the *in vitro* anti-proliferative activity and mechanistic studies. Mouse liver cancer xenograft model was established by subcutaneous inoculation of H22 cells into the right flank of mice. The tumor size and body weights of the mice were monitored and recorded every 2 days. Paclitaxel (PTX) was dosed as 8 mg/kg per 2 days (i.v.) due to its severe toxicity. To compare the anti-tumor efficacy of (\pm)-**19b** and CA-4, (\pm)-**19b** and CA-4 were dosed at 15 and 30 mg/kg per day (i.v.). None of the mice died in all groups after 21 days treatments. As shown in Figure 3A, both (\pm)-**19b** at the dose of 30 mg/kg per day and PTX at the dose of 8 mg/kg per 2 days significantly decreased the tumor volume. The reduction in tumor weight of PTX group reached 72.1% at 21 days after initiation of treatment as compared to vehicle, while (\pm)-**19b** reduced tumor weight by 46.5% and 62.3% at doses of 15 and 30 mg/kg per day (i.v.), respectively, which are more potent than CA-4 treatment groups (inhibitory rates of 44.8% and 55.3% at doses of 15 and 30 mg/kg per day, respectively) (Figure 3C). Importantly, (\pm)-**19b** did not significantly affect body weight even at the dose up to 30 mg/kg, while treat-

ment with PTX at a dose of 8 mg/kg per 2 days led to a significant decrease of body weight (Figure 3B). Thus, (\pm)-**19b** is worthy of further investigation for the treatment of cancers.

Finally, in order to investigate the effects of C-4 chirality on activity, the racemic mixture of (\pm)-**19b** were enantioseparated on a chiral column (see supporting information Figure S5) to afford (+)-**19b** and (-)-**19b**. Circular dichroism (CD) was performed to determine the absolute configuration, and the results indicated that the absolute configuration of (+)-**19b** is *R*-configured and the absolute configuration of (-)-**19b** is *S*-configured (see supporting information Figure S6).

Furthermore, (*R*)-(+)-**19b** and (*S*)-(-)-**19b** were evaluated for their anti-proliferative and inhibitory activities of tubulin polymerization. As shown in Table 1, the *R*-configured **19b** still exhibited very potent activity against five cancer cell lines, which were slightly potent than (\pm)-**19b**, whereas (*S*)-(-)-**19b** displayed a significant decrease of activity. As regard to the anti-tubulin assays, (*R*)-(+)-**19b** (IC_{50} = 2.5 μ M) was about 2-fold more potent than (*S*)-(-)-**19b** (IC_{50} = 4.3 μ M). Moreover, in assay of the colchicine competitive experiment, the binding ability of (*R*)-(+)-**19b** to the colchicine binding site was more potent than (\pm)-**19b**, and was comparable to that of CA-4 with the inhibition rates of 79.4% and 92.6% at 1 μ M and 5 μ M (Table S2).

To explain the significant difference in activity for two enantiomers of (\pm)-**19b**, molecular modeling studies were performed by using the DOCK program in Discovery Studio 3.0 software with the tubulin crystal structure (PDB: 5lyj). As a result, (*R*)-(+)-**19b** adopted a very similar positioning with that of CA-4. The phenolic hydroxyl and 4-methoxy of (*R*)-(+)-**19b** and CA-4 formed hydrogen bonds with Thr179 and Cys241 residues, respectively. The oxygen atom in isochromene ring interacted with residue Asn258 by a weak hydrogen bond (see Supporting Information Figure S7A). However, the binding pose of (*S*)-(-)-**19b** was flipped over 180° compared to that of CA-4, which may explain why both the anti-tubulin and anti-proliferative activity of (*S*)-(-)-**19b** decreased dramatically (Figure S7B).

In summary, a series of novel 4-arylisochromenes have been synthesized based on the structure of XJP-L (**8**). Anti-proliferative screening of these new synthesized compounds validated the representative compound (\pm)-**19b** as a high cytotoxic compound with IC_{50} ranging from 10 to 25 nM against a panel of cancer cell lines, which displayed a 1000-fold increase in activity compared with the lead **8**. It was found that (\pm)-**19b** also displayed potent inhibitory activity in tubulin polymerization assay (IC_{50} = 3.1 μ M). Further mechanism studies demonstrated that (\pm)-**19b** caused cell cycle arrest in the G2/M phase, induced cell apoptosis and depolarized mitochondria of K562 cells. And the immunofluorescent assay indicated that (\pm)-**19b** can effectively disrupt microtubule networks in a dose-dependent manner. The wound healing and tube formation assays also identified (\pm)-**19b** as a novel inhibitor of tubulin polymerization with potent vascular disrupting activity. Finally, the *in vivo* anti-tumor activity of (\pm)-**19b** was validated in H22 liver cancer xenograft mouse model, which is more potent than CA-4. Besides, (*R*)-(+)-**19b** and (*S*)-(-)-**19b** were obtained by chiral separation of (\pm)-**19b** and were evaluated for their anti-proliferative and anti-tubulin activities, respectively. (*R*)-(+)-**19b** was slightly more potent than (\pm)-**19b** whereas (*S*)-(-)-**19b** displayed a significantly decrease

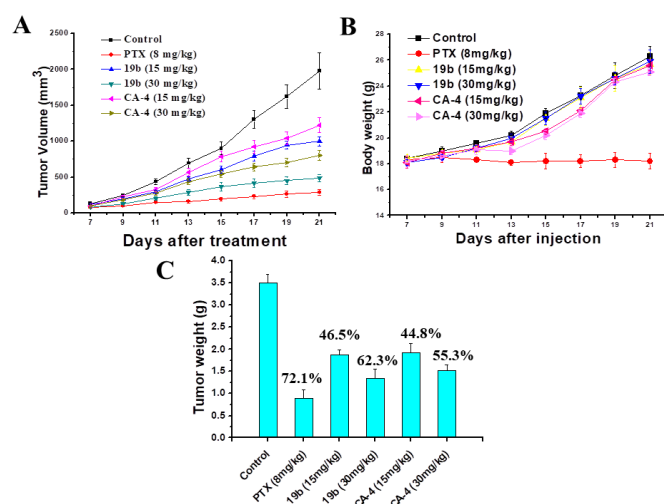


Figure 3. A) Tumor growth curves after injection with different formulations in H22 tumor bearing mice. B) Body weight changes of mice during treatment. C) (\pm)-**19b** treatment resulted in significantly lower tumor weight compared with controls.

of activity, which was further elucidated by molecular modeling studies. Altogether, (\pm)-**19b** may represent a novel class of anti-tubulin agent with potent anti-vascular and anti-tumor activities and deserves further investigation.

ASSOCIATED CONTENT

Supporting Information

Synthetic methods and characterization of target compounds, procedures for pharmacological activities. This material is available free of charge via the Internet at <http://pubs.acs.org>.

AUTHOR INFORMATION

Corresponding Authors

*E-mail addresses: jinyixu@china.com (J. Xu); cpujill@163.com (J. Liu); cpuxst@163.com (S. Xu).

ORCID

Jinyi Xu: 0000-0002-1961-0402

Author Contributions

The manuscript was written through contributions of all authors. All authors have given approval to the final version of the manuscript.

ACKNOWLEDGMENTS

This study was supported from the National Natural Science Foundation of China (No. 81673306, 81703348), The Open Project of State Key Laboratory of Natural Medicines, China Pharmaceutical University (No. SKLNMKF 201710), and China Postdoctoral Science Foundation (No. 2017100424) for financial support. The authors thank Dr. Dahong Li (Key Laboratory of Structure-Based Drug Design and Discovery of Ministry of Education and School of Traditional Chinese Materia Medica, Shenyang Pharmaceutical University, Shenyang, China) for the CD calculations.

Notes

The authors declare no competing financial interest.

ABBREVIATIONS

DMF, *N*, *N*-dimethylformamide; Xphos, 2-Dicyclohexylphosphino-2',4',6'-triisopropylbiphenyl; DCM, dichloromethane; THF, tetrahydrofuran; HUVECs, human umbilical vein endothelial cell.

Reference

- (1) Pettit, G. R.; Singh, S. B.; Hamel, E.; Lin, C. M.; Alberts, D. S.; Garcia-Kendal, D. Isolation and structure of the strong cell growth and tubulin inhibitor combretastatin A-4. *Experientia*. **1989**, *45*, 209-211.
- (2) Lin, C. M.; Singh, S. B.; Chu, P. S.; Dempcy, R. O.; Schmidt, J. M.; Pettit, G. R.; Hamel, E. Interactions of tubulin with potent natural and synthetic analogs of the antimetabolic agent combretastatin: a structure-activity study. *Mol. Pharmacol.* **1988**, *34*, 200-208.
- (3) Dark, G. G.; Hill, S. A.; Prise, V. E.; Tozer, G. M.; Pettit, G. R.; Chaplin, D. J. Combretastatin A-4, an agent that displays potent and selective toxicity toward tumor vasculature. *Cancer Res.* **1997**, *57*, 1829-1834.

- (4) Pérez-Pérez, M. J.; Priego, E. M.; Bueno, O.; Martins, M. S.; Canela, M. D.; Liekens, S. Blocking blood flow to solid tumors by destabilizing tubulin: An approach to targeting tumor growth. *J. Med. Chem.* **2016**, *59*, 8685-8711.
- (5) Porcù, E.; Bortolozzi, R.; Basso, G.; Viola, G. Recent advances in vascular disrupting agents in cancer therapy. *Future Med. Chem.* **2014**, *6*, 1485-1498.
- (6) Jaroch, K.; Karolak, M.; Górski, P.; Jaroch, A.; Krajewski, A.; Ilnicka, A.; Sloderbach, A.; Stefański, T.; Sobiak, S. Combretastatins: In vitro structure-activity relationship, mode of action and current clinical status. *Pharmacol. Rep.* **2016**, *68*, 1266-1275.
- (7) Ji, Y.; Liu, Y.; Liu, Z.; Tubulin colchicine binding site inhibitors as vascular disrupting agents in clinical developments. *Curr. Med. Chem.* **2015**, *22*, 1348-1360.
- (8) <http://clinicaltrials.gov>: (a) Focus: PCC + Bevacizumab + CA4P Versus PCC + Bevacizumab + Placebo for subjects with platinum resistant Ovarian Cancer; (b) Safety and effectiveness of Combretastatin A-4 phosphate combined with chemotherapy in advanced solid tumors; (c) Foscarnet or Placebo in combination with Carboplatin/Paclitaxel in Anaplastic Thyroid Cancer.
- (9) <http://investor.mateon.com/releasedetail.cfm?ReleaseID=1041745>.
- (10) Aprile, S.; Del Grosso, E.; Tron, G. C.; Grosa, G. In vitro metabolism study of combretastatin A-4 in rat and human liver microsomes. *Drug Metab. Dispos.* **2007**, *35*, 2252-2261.
- (11) Li, W.; Sun, H.; Xu, S.; Zhu, Z.; Xu, J. Tubulin inhibitors targeting the colchicine binding site: a perspective of privileged structures. *Future Med. Chem.* **2017**, *9*, 1765-1794.
- (12) Kaur, R.; Kaur, G.; Gill, R. G.; Soni, R.; Bariwal, J. Recent developments in tubulin polymerization inhibitors: An overview. *Eur. J. Med. Chem.* **2014**, *87*, 89-124.
- (13) Lu, Y.; Chen, J.; Xiao, M.; Li, W.; Miller, D. An overview of tubulin inhibitors that interact with the colchicine binding site. *Pharm. Res.* **2012**, *29*, 2943-2971.
- (14) Sriram, M.; Hall, J. J.; Grohmann, N. C.; Strecker, T. E.; Wootton, T.; Franken, A.; Trawick, M. L.; Pinney, K. G. Design, synthesis and biological evaluation of dihydronaphthalene and benzosuberene analogs of the combretastatins as inhibitors of tubulin polymerization in cancer chemotherapy. *Bioorg. Med. Chem.* **2008**, *16*, 8161-8171.
- (15) Herdman, C. A.; Strecker, T. E.; Tanpure, R. P.; Chen, Z.; Winters, A.; Gerberich, J.; Liu, L.; Hamel, E.; Mason, R. P.; Chaplin, D. J.; Trawick, M. L.; Pinney, K. G. Synthesis and biological evaluation of benzocyclooctene-based and indene-based anticancer agents that function as inhibitors of tubulin polymerization. *Med. Chem. Comm.* **2012**, *7*, 2418-2427.
- (16) Pinney, K. G.; Mocharla, V. P.; Chen, Z.; Garner, C. M.; Ghatak, A.; Hadimani, M.; Kessler, J.; Dorsey, J. M.; Edvardsen, K.; Chaplin, D. J.; Prezioso, J.; Ghatak, U. R. Tubulin binding agents and corresponding prodrug constructs. US20040043969-A1, 2004.
- (17) Pinney, K. G.; Mocharla, V. P.; Chen, Z.; Garner, C. M.; Ghatak, A.; Hadimani, M.; Kessler, J.; Dorsey, J. M.; Edvardsen, K.; Chaplin, D. J.; Prezioso, J.; Ghatak, U. R. Tubulin

binding agents and corresponding prodrug constructs: U.S. Patent 7001926, Feb 21, 2006.

(18) Devkota, L.; Lin, C.; Strecker, T. E.; Wang, Y.; Tidmore, J. K.; Chen, Z.; Guddneppanavar, R.; Jelinek, C. J.; Lopez, R.; Liu, L.; Hamel, E.; Mason, R.; Chaplin, D. J.; Trawick, M. L.; Pinney, K. G. Design, synthesis, and biological evaluation of water-soluble amino acid prodrug conjugates derived from combretastatin, dihydronaphthalene, and benzosuberene-based parent vascular disrupting agents. *Bioorg. Med. Chem.* **2016**, *24*, 938-956.

(19) Rasolofonjatovo, E.; Provot, O.; Hamze, A.; Rodrigo, J.; Bignon, J.; Wdzieczak-Bakala, J.; Destravines, D.; Dubois, J.; Brion, J.; Alami, M. Conformationally restricted naphthalene derivatives type isocombreastatin A-4 and isoerianin analogues: synthesis, cytotoxicity and antitubulin activity. *Eur. J. Med. Chem.* **2012**, *52*, 22-32.

(20) Yan, J.; Hu, J.; An, B.; Huang, L.; Li, X. Design, synthesis, and biological evaluation of cyclic-indole derivatives as antitumor agents via the inhibition of tubulin polymerization. *Eur. J. Med. Chem.* **2017**, *125*, 663-675.

(21) Galli, U.; Travelli, C.; Aprile, S.; Arrigoni, E.; Torretta, S.; Giosa, G.; Massarotti, A.; Sorba, G.; Canonico, P. L.; Genazzani, A. A.; Tron, G. C. Design, synthesis, and biological evaluation of combretabenzodiazepines: a novel class of anti-tubulin agents. *J. Med. Chem.* **2015**, *58*, 1345-1357.

(22) Yao H.; Liu J.; Xu S.; Zhu Z.; Xu J. The structural modification of natural products for novel drug discovery. *Expert Opin. Drug Discov.* **2017**, *12*, 121-140.

(23) Qian, H.; Huang, W. L.; Wu, X. M.; Zhang, H. B.; Zhou, J. P.; Ye, W. C. A new isochroman-4-one derivative from the peel of *Musa sapientum* L. and its total synthesis. *Chin. Chem. Lett.* **2007**, *18*, 1227-1230.

(24) Liu, J.; Ren, H.; Xu, J.; Bai, R.; Yan, Q.; Huang, W.; Wu, X.; Fu, J.; Wang, Q.; Wu, Q.; Fu, R. Total synthesis and antihypertensive activity of (\pm) 7, 8-dihydroxy-3-methyl-isochro-

-man-4-one. *Bioorg. Med. Chem. Lett.* **2009**, *19*, 1822-1824.

(25) Fu, R.; Chen, Z.; Wang, Q.; Guo, Q.; Xu, J.; Wu, X. XJP-1, a novel ACEI, with anti-inflammatory properties in HU-VECs. *Atherosclerosis*. **2011**, *219*, 40-48.

(26) Fu, R.; Wang, Q.; Guo, Q.; Xu, J.; Wu, X. XJP-1 protects endothelial cells from oxidized low-density lipoprotein-induced apoptosis by inhibiting NADPH oxidase subunit expression and modulating the PI3K/Akt/eNOS pathway. *Vasc. Pharmacol.* **2013**, *58*, 78-86.

(27) Negi, A. S.; Gautam, Y.; Alam, S.; Chanda, D.; Luqman, S.; Sarkar, J.; Khan, F.; Konwar, R.; Natural antitubulin agents: Importance of 3,4,5-trimethoxyphenyl fragment. *Bioorg. Med. Chem.* **2015**, *23*, 373-3891.

(28) Dong, M.; Liu, F.; Zhou, H.; Zhai, S.; Yan, B. Novel natural product and privileged scaffold-based tubulin inhibitors targeting the colchicine binding site. *Molecules* **2016**, *21*, 1375.

(29) Li, L.; Jiang, S.; Li, X.; Liu, Y.; Su, J.; Chen, J. Recent advances in trimethoxyphenyl (TMP) based tubulin inhibitors targeting the colchicine binding site. *Eur. J. Med. Chem.* **2018**, *151*, 482-494.

(30) Wang, C.; Wu, Z.; Wang, J.; Liu, J.; Yao, H.; Lin, A.; Xu, J. An efficient synthesis of 4-isochromanones via parham-type cyclization with weinreb amide. *Tetrahedron*. **2015**, *71*, 8172-8177.

(31) Dumontet, C.; Jordan, M. A. Microtubule-binding agents: a dynamic field of cancer therapeutics. *Nat. Rev. Drug Discov.* **2010**, *9*, 790-803.

(32) Schwartz, E. L. Antivascular actions of microtubule-binding drugs. *clin. Cancer Res.* **2009**, *15*, 2594-2601.

(33) Siemann, D. W.; Bibby, M. C.; Dark, G. G.; Dicker, A. P.; Eskens, F. A.L.M.; Horsman, M. R.; Marme, D.; LoRusso, P. M. Differentiation and definition of vascular-targeted therapies. *Clin. Cancer Res.* **2005**, *11*, 416-420.

Table of Contents

